Optical properties of silicon nanowires from cathodoluminescence imaging and time-resolved photoluminescence spectroscopy

M. Dovrat,[1] N. Arad,[1] X.-H. Zhang,[2] S.-T. Lee,[2,3] and A. Sa'ar[1,*]

[1]*Racah Institute of Physics and the Center for Nanoscience and Nanotechnology, The Hebrew University of Jerusalem, Israel*

[2]*Nano and Organic Photoelectronic Laboratory, Technical Institute of Physics and Chemistry, Chinese Academy of Sciences, Beijing, China*

[3]*Center for Super-Diamond and Advanced Films and Department of Physics and Materials Science, City University of Hong Kong, Hong Kong SAR, China*

(Received 3 November 2006; revised manuscript received 6 March 2007; published 30 May 2007)

Time-resolved photoluminescence spectroscopy and cathodoluminescence spectroscopy and imaging have been used to investigate the optical properties of oxygen- and hydrogen-terminated silicon nanowires. We have found that the red- and the blue-emission bands from these nanowires are characterized by homogeneous broadening and are due to interface states in the silicon core and oxygen-based defects at the oxide cladding layer, respectively. Our results exclude the possibility that quantum confinement effects are responsible for these emission bands.

DOI: 10.1103/PhysRevB.75.205343 PACS number(s): 78.67.Lt, 78.60.Hk, 68.37.Hk

I. INTRODUCTION

Silicon-based nanostructures, such as porous silicon[1–3] (PS), silicon nanocrystals[4] (SiNCs), and silicon nanowires[5–15] (SiNWs), have attracted much attention due to the discovery that these nano-objects can emit visible light quite efficiently. This topic has been the subject of extensive research over the past decade since the bulk silicon crystal is known to be an indirect band-gap semiconductor and a poor emitter of light even at low temperatures. It has been suggested that quantum confinement (QC) effects combined with surface phenomena are responsible for the photoluminescence (PL) from SiNCs and PS.[16–19] However, the applicability of these models and explanations to the case of SiNWs is not clear, as there are much less experimental works and literature about the optical properties of these one-dimensional silicon nano-objects.[6,12–15] In particular, it is quite difficult to decide if the luminescence from SiNWs is due to QC effects or comes from local defects and interface states, especially since the distribution of diameters and sizes of the nanowires might screen quantum size effects. Hence, the ability to study the optical properties of individual SiNWs can provide important information for resolving this issue.

In this work, we report on cathodoluminescence (CL) spectroscopy and imaging and time-resolved PL spectroscopy of individual SiNWs, terminated by both oxygen (O) and hydrogen (H) surface bonds. Our results indicate that the origin of the luminescence from moderate size SiNWs (diameter $\gtrsim$10 nm) cannot be assigned directly to QC but rather to surface radiative recombination centers located at the interface between the silicon core and the cladding material of the nanowires. In addition, we have found that the broadening mechanism responsible for the emission lines should be related to homogeneous broadening of individual SiNWs rather than to inhomogeneous characteristics of the ensemble system such as the distribution of diameters and sizes of SiNWs.

II. EXPERIMENT

SiNWs were prepared by the oxide-assisted growth method,[8] where a target of silicon monoxide (SiO) has been used to initiate the growth of SiNWs. The SiO powder was heated up to 1200 °C under the flow of mixed argon and hydrogen gases to form SiNWs downstream in an evacuated alumina tube. The as-grown SiNWs have a core-shell structure with outer diameters in the range of 20–50 nm and are composed of a crystalline silicon core (about 2/3 of the outer diameter) and a silicon dioxide (SiO_2) shell, as confirmed by transmission electron microscopy[10] and scanning tunneling microscopy.[5] For our experiments, the SiNWs were mechanically pressed to the surface of a silicon substrate, thus providing good mechanical support to the SiNWs. In order to remove the oxide cladding and to form hydrogen-terminated SiNWs, the samples were etched by an aqueous solution of 5% HF for 10 min until most of the silicon-oxygen bonds disappeared. This has been confirmed by infrared absorption spectroscopy using a Fourier-transform infrared (FTIR) spectrometer. The FTIR spectra are shown in Fig. 1, where the

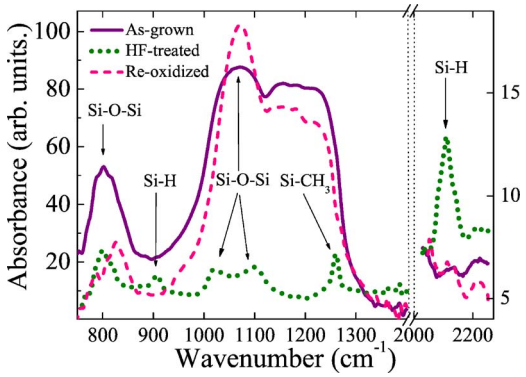

FIG. 1. (Color online) Infrared absorption spectra of the as-grown, HF-treated, and HF-treated and reoxidized SiNWs. The arrows mark the position of the various silicon-oxygen and silicon-hydrogen vibration modes.

various silicon-oxygen and silicon-hydrogen vibration modes[11,20–23] are marked by arrows. We notice that the silicon-oxygen absorption bands (at 1070–1220 and at 800 and 820 cm^{-1}) fade out after HF treatment, while the silicon-hydrogen absorption bands (at 2100 and 910 cm^{-1}) are not present for as-grown and for HF-treated SiNWs that were subsequently dry oxidized for 240 min at 700 °C. In order to avoid further oxidation, the HF-treated SiNWs were kept in a vacuum cryostat for the rest of the experiments.

For CL measurements we have used a high-resolution scanning electron microscope (HRSEM) (FEI Sirion) equipped with the Gatan MonoCL3 system. This system includes a parabolloidal mirror introduced into the scanning electron microscope (SEM) chamber for collecting the light into a 1/3 m optical monochromator and a cooled GaAs photomultiplier to detect the optical signal for obtaining either the CL spectrum or a CL image (by feeding back the signal into the SEM). For panchromatic CL imaging, we have detected the emitted light by bypassing the monochromator, while for quasimonochromatic CL imaging, we used a set of color processing filters. A Gatan continuous flow liquid-He stage was used to perform the experiments in the 5–300 K temperature range. For cw and time-resolved PL experiments, an Ar^+ laser operating at 457.9 nm has been used as the source of excitation while an acousto-optic modulator has been used to modulate the laser beam. The PL signal was dispersed by a 1/4 m monochromator, detected by a photomultiplier, and analyzed by a gated photon counting system. The samples were placed in an optical cryostat that allows cooling the samples down to 77 K.

III. RESULTS

SEM images of the as-grown SiNWs are shown in Figs. 2(a) and 2(b). The image of Fig. 2(a) reveals a typical bundle of SiNWs, a few microns in length, while Fig. 2(b) shows a higher magnification of several SiNWs near the edge of the sample. Figure 2(c) presents the corresponding room-temperature panchromatic CL image of the SiNWs. A clear correlation between the SEM image [Fig. 2(b)] and the CL image [Fig. 2(c)] has been obtained, indicating that the CL emission originates from the SiNWs. In Fig. 2(b), a rectangular region containing an individual SiNW has been marked. The CL spectra of the entire O-terminated (as-grown) SiNWs bundle and the individual SiNW are presented in Fig. 3. Both spectra reveal essentially the same features of a narrow red-emission band centered at ~1.94 eV (640 nm) and a second broader blue-emission band at ~2.65 eV (470 nm). Additionally, the red-emission band exhibits a shoulder on the low-energy side (separated by approximately 0.1 eV from the peak), clearly visible in the bulk spectrum. The CL signal characteristics were found to be independent of temperature in the range of 5–300 K. We would like to emphasize that the same peak energies and approximately the same linewidths have been observed for the individual SiNW and the entire bundle of SiNWs, with the only difference being the lower signal intensity obtained for the individual SiNW (particularly for the red-emission line). This result suggests that the CL spectra should be associated with the homogeneous characteristics of the SiNWs rather than inhomogeneous characteristics associated with size and diameter distribution of the SiNWs.

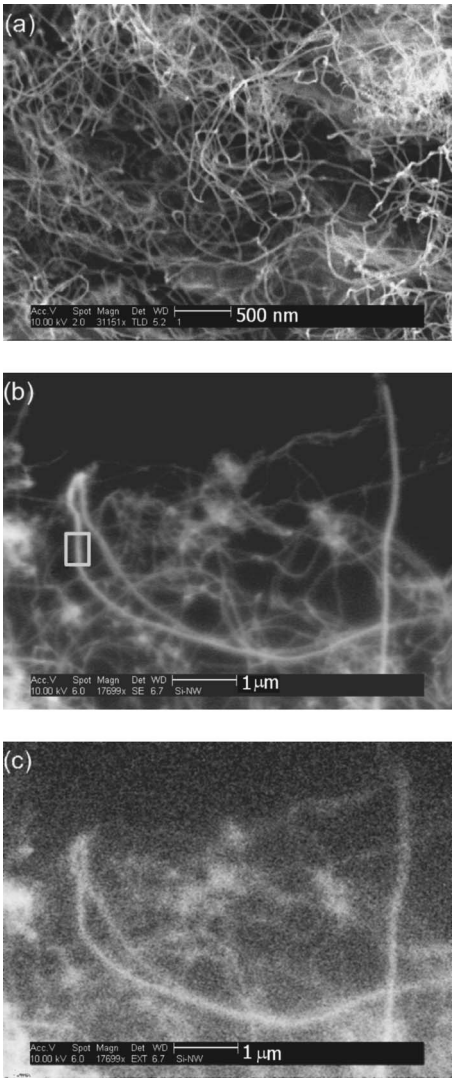

FIG. 2. (a) A SEM image of a bundle of SiNWs. (b) A SEM image of a few SiNWs near the edge of the sample. A rectangular region containing an individual SiNW has been marked. (c) The corresponding panchromatic CL image of the SiNWs shown in (b).

In order to resolve the origin of each of the emission bands shown in Fig. 3, we have performed room-temperature quasimonochromatic CL imaging of a single SiNW. The results of this experiment are shown in Fig. 4. In Fig. 4(a), we present an HRSEM image of a section of two SiNWs near the edge of the sample, where they could be separated and distinguished from the rest of the "bulky" area of SiNWs. The image reveals the fine structure of the left SiNW, which is composed of small segments along the wire axis, as observed elsewhere.[24] The chain of segments has an average diameter of 73 nm, while the narrower right SiNW in the image has an average diameter of 63 nm. The corresponding quasimonochromatic CL images, using red and blue filters, are shown in Figs. 4(b) and 4(c), respectively (the corresponding transmittance ranges of these filters are shown by the horizontal bars at the top of Fig. 3). Here again, the

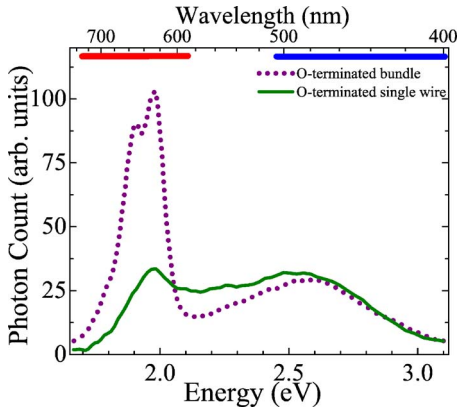

FIG. 3. (Color online) CL spectra of the bundle of O-terminated (as-grown) SiNWs shown in Fig. 2(a) and the rectangular region containing an individual SiNW shown in Fig. 2(b). The horizontal bars at the top represent the transmittance regions of the red and blue color filters used for quasimonochromatic CL imaging (see Fig. 4).

correlation between the HRSEM and the CL images is evident. In addition, one can see that the width of the "blue" CL image is larger than the width of the "red" CL image. This result has been quantified in Fig. 5, where the CL intensity profiles, obtained by averaging along several cross sections of the SiNWs, are shown. The CL intensity profiles have been fitted into a Gaussian form (represented by the solid lines) with a full width at half maximum of 54±3 nm (red band) and 63±3 nm (blue band), respectively. These diameters of the SiNW should be compared to the width measured using the SEM image of Fig. 5(a) by the same procedure (63±2 nm). These values should not be considered as the true width of the SiNWs, as certain broadening mechanisms related to the electron-beam size and energy[25] increase their width. Yet, we argue that the significant difference between the red and the blue CL widths (~10 nm) is an indication that these emission lines originate from different layers of the SiNWs, as schematically illustrated in the inset to Fig. 5. We assign the blue band to the oxide layer that encapsulates the silicon core of the wires, while the red band is assigned to the interface between the silicon core and the oxide cladding, as will be discussed hereafter.

In contrast to the CL spectra of the as-grown SiNWs, we could not observe any CL signal from the HF-treated hydrogen-terminated SiNWs. On the other hand, after reoxidation of the HF-treated SiNWs, the CL spectra and images, shown in Figs. 2–5, reproduce themselves. Hence, we conclude that only oxygen-terminated SiNWs can produce CL emission, while hydrogen-terminated SiNWs cannot.

Next, we discuss results obtained from cw and time-resolved PL spectroscopy. The cw PL spectra of the as-grown, HF-treated, and reoxidized SiNWs are shown in Fig. 6(a), revealing a strong, red-emission band. However, this red PL emission band is broader and is redshifted relative to the CL red band to about 1.77 eV (700 nm). In contrast to the CL experiment, HF treatment did not produce any significant change in the PL spectrum of the SiNWs. Figure 7 presents typical time-resolved decay curves, at various photon energies, of the as-grown and the HF-treated SiNWs. All decay curves are best described by a stretched-exponential decay function, $I=I_0 \exp[-(t/\tau)^{\beta}]$, similar to results obtained for PS (Ref. 1) and SiNCs.[26–29] The PL decay time τ for the various types of SiNWs is shown in Fig. 6(b). The stretching exponent, $\beta \approx 0.8 \pm 0.1$, has been found to be approximately the same for all samples and photon energies. Here again, we find a significant distinction between the O-terminated SiNWs (i.e., as-grown and reoxidized SiNWs) and the H-terminated SiNWs. While the PL lifetime of the O-terminated SiNWs has been found to be rather slow, in the order of ~1 ms, with a relatively weak dependence on the photon energy, the PL decay time of the H-terminated SiNWs is much faster, in the order of ~10 μs. In addition,

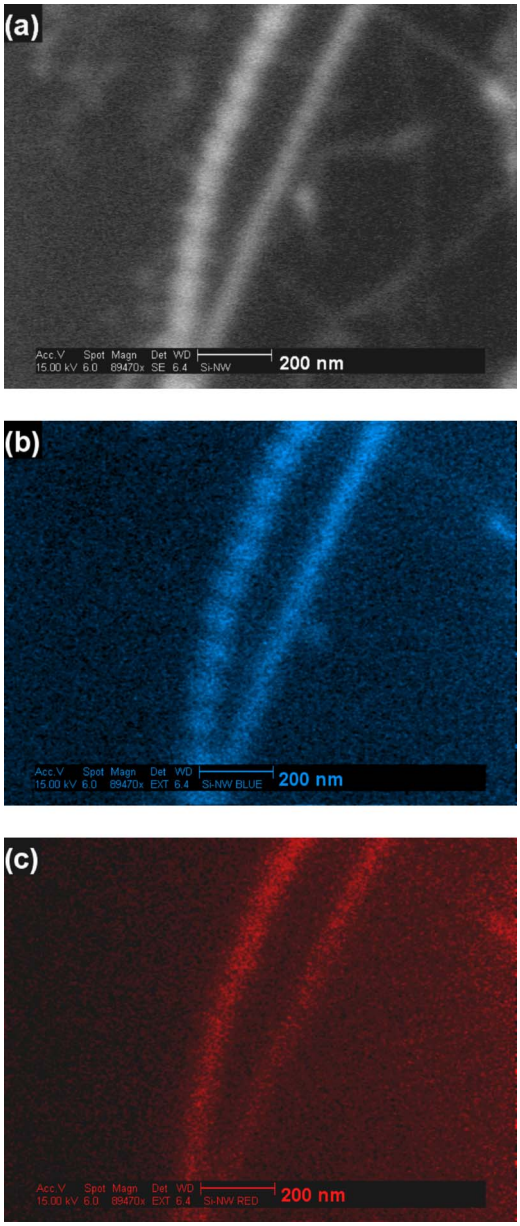

FIG. 4. (Color online) (a) HRSEM image of single SiNWs. (b) The corresponding pseudocolor blue CL image of the same SiNWs. (c) The corresponding pseudocolor red CL image. The transmittance of the filters is shown by the bars at the top of Fig. 3.

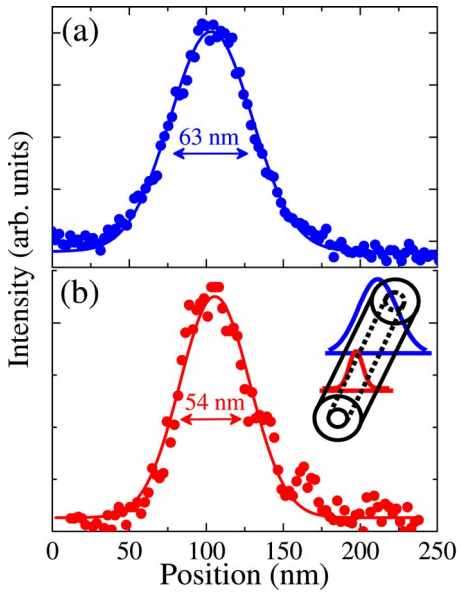

FIG. 5. (Color online) Quasimonochromatic CL intensity profiles of the right SiNW presented in Fig. 4. (a) The intensity profile in the blue CL image [Fig. 4(b)]. (b) The intensity profile in the red CL image [Fig. 4(c)]. Inset: A schematic illustration of the core-clad structure of the SiNWs and the corresponding blue (top) and red (bottom) emission lines.

we have found the PL decay times to be essentially independent of temperature (77–300 K) for both samples.

IV. DISCUSSION

In order to explain the origin of the luminescence lines from SiNWs, we would like to emphasize that quantum confinement cannot be responsible for these emission bands. In

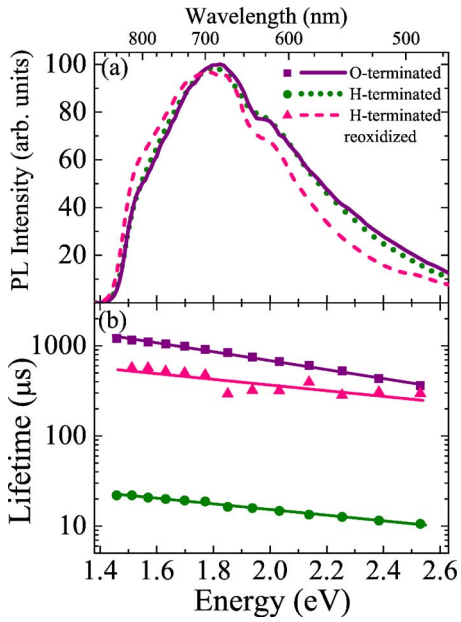

FIG. 6. (Color online) (a) PL specta and (b) PL lifetimes of O-terminated, H-terminated, and reoxidized SiNWs.

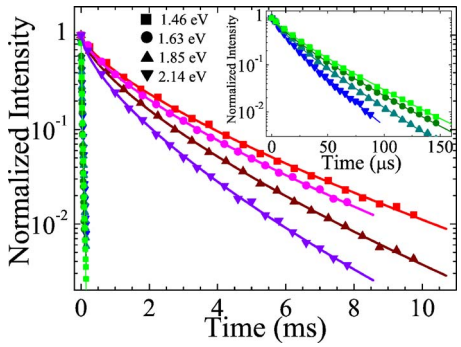

FIG. 7. (Color online) Normalized PL intensity versus time for O-terminated (slow decays) and H-terminated (fast decays) SiNWs at several photon energies. The inset is an expansion of the time scale to show the fast decays of H-terminated SiNWs. The solid lines are fits to the stretched-exponential decay function (see text).

SiNCs, QC appears to dominate for nanocrystals smaller than 5–6 nm, when the size of the nanocrystals becomes comparable to or smaller than the excitonic radius of the electron-hole pairs. The diameter of the SiNWs studied here is about 20–50 nm, much larger than the excitonic radius (this conclusion holds even if one takes the diameter of the silicon core to be ~1/3 of the overall diameter). Other indications that do not favor the QC model are the weak dependence of the PL lifetime on the photon energy, as opposed to SiNCs,[26] the homogeneous broadening of the CL spectra despite the fairly broad size distribution of the SiNWs, and the disappearance of CL emission with HF treatment.

We notice that HF treatment of SiNWs results in etching of the oxide cladding layer as well as replacement of silicon-oxygen bonds on the surface of the silicon core with silicon-hydrogen and silicon-hydroxyl bonds. While PL has been observed for O- and H-terminated SiNWs, CL has been observed only for O-terminated SiNWs in our experiment. A similar behavior of CL emission bands was found for oxidized PS and was attributed to oxygen defects in the PS medium.[30] CL blue- and red-emission bands (at ~2.6 and ~1.8–1.9 eV, respectively) were observed both for PS (Ref. 31) and silica nanowires[32] and were assigned to various oxygen-related defects.

This picture of oxygen-related radiative centers in the oxide cladding layer explains the disappearance of the CL blue band from H-terminated SiNWs after the oxide cladding is removed by HF. On the other hand, the red-emission bands (CL and PL) cannot be associated with the oxide cladding alone, as H-terminated SiNWs do exhibit the red PL emission band.

Our quasimonochromatic CL imaging results suggest that the red band originates from radiative centers at the interface of the silicon core (a similar result was obtained by Sham *et al.*[12]). However, The much faster PL lifetime of H-terminated SiNWs, by about 2 orders of magnitude, compared to O-terminated SiNWs suggests that different types of radiative mechanisms contribute to either case (despite the similarity between the PL spectra). The fact that HF treatment removes the silicon-oxygen bonds at the core-clad interface of SiNWs and replaces them with silicon-hydrogen and silicon-hydroxyl bonds, known to be unstable under e-beam

radiation, might explain the quenching of the red band at ~1.9 eV from the CL spectra of H-terminated SiNWs. Note also that the role of hydrogen- and oxygen-terminated bonds at the surface of SiNCs have been reported lately,[17–19] particularly the faster dynamics associated with hydrogen and hydroxyl surface bonds.

V. CONCLUSIONS

In conclusion, CL spectroscopy and imaging of individual SiNWs and time-resolved PL spectroscopy indicate that the origin of the luminescence from moderate size SiNWs (20–50 nm) comes from interface states and radiative centers in the cladding layer of the SiNWs. These luminescence bands may also exist in small-diameter SiNWs and could screen luminescence bands that arise from QC. Hence, a careful analysis of the luminescence spectra, particularly the dependence on the size of the SiNWs, is required in order to conclude about the presence of quantum size effects in SiNWs.

ACKNOWLEDGMENTS

This work was supported by a joint Chinese-Israeli research grant provided by the ministries of science of both countries and by Grant No. 422/04 of the Israel Science Foundation (ISF). S.T.L. acknowledges the support by the Research Grants Council of Hong Kong (Project No. CityU 3/04C), China.

*Electronic address: saar@vms.huji.ac.il

[1] *Light Emission in Silicon: From Physics to Devices*, edited by D. J. Lockwood (Academic, New York, 1998).
[2] O. Bisi, S. Ossicini, and L. Pavesi, Surf. Sci. Rep. **38**, 1 (2000).
[3] A. G. Cullis, L. T. Canham, and P. D. J. Calcott, J. Appl. Phys. **82**, 909 (1997).
[4] A. G. Nassiopoulou, in *Encyclopedia of Nanoscience and Nanotechnology*, edited by H. S. Nalwa (American Scientific, Stevenson Ranch, CA, 2004), Vol. 9, pp. 793–813.
[5] D. D. D. Ma, C. S. Lee, F. C. K. Au, S. Y. Tong, and S. Lee, Science **299**, 1874 (2003).
[6] D. D. D. Ma, S. T. Lee, and J. Shinar, Appl. Phys. Lett. **87**, 033107 (2005).
[7] Y. Cui and C. M. Lieber, Science **291**, 851 (2001).
[8] R. Q. Zhang, Y. Lifshitz, and S. T. Lee, Adv. Mater. (Weinheim, Ger.) **15**, 635 (2003).
[9] A. M. Morales and C. M. Lieber, Science **279**, 208 (1998).
[10] C.-P. Li, C. S. Lee, X. L. Ma, N. Wang, R. Q. Zhang, and S. T. Lee, Adv. Mater. (Weinheim, Ger.) **15**, 607 (2003).
[11] X. Sun, S. Wang, N. Wong, D. Ma, B. Lee, and S. T. Teo, Inorg. Chem. **42**, 2398 (2003).
[12] T. K. Sham, S. J. Naftel, P.-S. G. Kim, R. Sammynaiken, Y. H. Tang, I. Coulthard, A. Moewes, J. W. Freeland, Y.-F. Hu, and S. T. Lee, Phys. Rev. B **70**, 045313 (2004).
[13] X. H. Sun, N. B. Wong, C. P. Li, S. T. Lee, and T. K. Sham, J. Appl. Phys. **96**, 3447 (2004).
[14] S. Bhattacharya, D. Banerjee, K. W. Adu, S. Samui, and S. Bhattacharyya, Appl. Phys. Lett. **85**, 2008 (2004).
[15] Z. Zhang, X. Wu, J. Shen, L. Yang, Y. Shi, P. K. Chu, and G. Siu, J. Cryst. Growth **285**, 620 (2005).
[16] M. V. Wolkin, J. Jorne, P. M. Fauchet, G. Allan, and C. Delerue, Phys. Rev. Lett. **82**, 197 (1999).
[17] G. Allan and C. Delerue, Phys. Rev. B **66**, 233303 (2002).
[18] A. Sa'ar, Y. Reichman, M. Dovrat, D. Krapf, J. Jedrzejewski, and I. Balberg, Nano Lett. **5**, 2443 (2005).
[19] A. Sa'ar, M. Dovrat, J. Jedrzejewski, and I. Balberg, Physica E (Amsterdam) **38**, 122 (2007).
[20] W. Theiß, Surf. Sci. Rep. **29**, 91 (1997).
[21] K. T. Queeney, M. K. Weldon, J. P. Chang, Y. J. Chabal, A. B. Gurevich, J. Sapjeta, and R. L. Opila, J. Appl. Phys. **87**, 1322 (2000).
[22] M. A. Holland, D. M. Pickup, G. Mountjoy, G. W. Tsang, E. S. C. Wallidge, R. J. Newport, and M. E. Smith, J. Mater. Chem. **10**, 2495 (2000).
[23] C. Vautrin-Ul, F. Roux, C. Boisse-Laporte, A. Pastol, and J. L. Chausse, J. Mater. Chem. **12**, 2318 (2002).
[24] H. Y. Peng, Z. W. Pan, L. Xu, X. H. Fan, N. Wang, C. S. Lee, and S. T. Lee, Adv. Mater. (Weinheim, Ger.) **13**, 317 (2001).
[25] P. Echlin, C. Fiori, J. Goldstein, D. C. Joy, and D. E. Newbury, *Advanced Scanning Electron Microscopy and X-Ray Microanalysis* (Plenum, New York, 1986).
[26] M. Dovrat, Y. Goshen, J. Jedrzejewski, I. Balberg, and A. Sa'ar, Phys. Rev. B **69**, 155311 (2004).
[27] O. Guillois, N. Herlin-Boime, C. Reynaud, G. Ledoux, and F. Huisken, J. Appl. Phys. **95**, 3677 (2004).
[28] A. Y. Kobitski, K. S. Zhuravlev, H. P. Wagner, and D. R. T. Zahn, Phys. Rev. B **63**, 115423 (2001).
[29] J. Linnros, N. Lalic, A. Galeckas, and V. Grivickas, J. Appl. Phys. **86**, 6128 (1999).
[30] O. Arakaki, A. Hatta, T. Ito, and A. Hiraki, Jpn. J. Appl. Phys., Part 1 **33**, 6586 (1994).
[31] G. M. Williams, in *Properties of Porous Silicon*, edited by L. T. Canham (INSPEC, London, 1997), pp. 270–275.
[32] N. G. Shang, U. Vetter, I. Gerhards, H. Hofsäss, C. Ronning, and M. Seibt, Nanotechnology **17**, 3215 (2006).